Accepted Manuscript

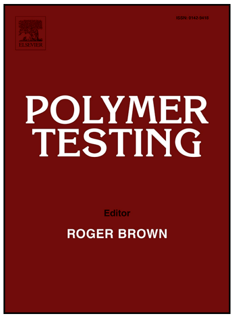

Effect of crumb rubber on mechanical properties of multi-phase syntactic foams

Thong M. Pham, Jim Kingston, Gary Strickland, Wensu Chen, Hong Hao

PII: S0142-9418(17)31374-0

DOI: 10.1016/j.polymertesting.2017.12.033

Reference: POTE 5285

To appear in: *Polymer Testing*

Received Date: 24 September 2017

Revised Date: 6 November 2017

Accepted Date: 30 December 2017

Please cite this article as: T.M. Pham, J. Kingston, G. Strickland, W. Chen, H. Hao, Effect of crumb rubber on mechanical properties of multi-phase syntactic foams, *Polymer Testing* (2018), doi: 10.1016/j.polymertesting.2017.12.033.

Effect of Crumb Rubber on Mechanical Properties of Multi-phase Syntactic Foams

Thong M. Pham[1], Jim Kingston[2], Gary Strickland[2], Wensu Chen[1] and Hong Hao[1*]

[1]Center for Infrastructural Monitoring and Protection, School of Civil and Mechanical Engineering, Curtin University, Kent Street, Bentley, WA 6102, Australia

[2] Matrix Composites & Engineering, 150 Quill Way, Henderson, WA 6166, Australia

[*]Corresponding author's email: hong.hao@curtin.edu.au

Abstract

Syntactic foam is a lightweight and strong material which can be used in marine and aeronautical applications. However, the brittleness of the material limits its application to a broader range. Adding crumb rubber to the syntactic foam can increase its energy absorption capacity. The effect of crumb rubber on the fracture toughness and energy absorption capacity of 2-phase and 3-phase syntactic foam is evaluated under both static and impact loads. The experimental results have shown that the fracture toughness of the 2-phase rubberized syntactic foam increased by 8% while an increase of 22% of its fracture energy was observed. Under quasi-static loads, the 3-phase rubberized syntactic foam showed decreases in the compressive strength and elastic modulus but an increase in the energy absorption capacity as compared to the syntactic foam without crumb rubber. In addition, the impact energy absorption of the 3-phase rubberized syntactic foam increased by 24% as compared to that of the 3-phase syntactic foam without crumb rubber.

Keywords: Syntactic foam; Impact behaviour, Energy absorption; Fracture toughness; Crumb rubber.

1. Introduction

Syntactic foam is a type of lightweight and rigid composite material, which consists of binder and fillers. The binder matrix can be made of polymeric resin, metal and ceramic [1] and the fillers are in forms of microsphere and macro-sphere, which are made from rigid materials such as glass, carbon, metal, ceramic, cenosphere and polymeric materials [2]. The syntactic foams are commonly categorized as 2-phase and 3-phase [3]. It is noted that this classification is based on the main compositions of the material regardless the additive (e.g. crumb rubber). Traditional foam is mainly made of binder matrix with relatively low compressive strength. Therefore, microspheres are mixed with binder matrix to form the 2-phase syntactic foam. 3-phase syntactic foam is made of microspheres mixed binder matrix dispersed with macro-spheres, which can be gaseous voids or hollow spheres [4]. The macro-sphere, as reinforcing filler of syntactic foam, can be made of spheres coated with fibre reinforced epoxy. For instance, Wu et al. [3] developed a macro-sphere by coating Expanded Polystyrene (EPS) beads with carbon fibre reinforced epoxy using rolling ball method.

The superior mechanical properties of the syntactic material can be obtained through the composite action [5-7]. It should be noted that the effect of the volume fraction of microsphere on the mechanical properties of syntactic foam is not well understood [8, 9]. Swetha and Kumar [2] found that the strength of the foam decreased with the increase of microsphere content. Its energy absorption capacity kept increasing with the rising content of microsphere up to 40% and then decreased. Kim and Khamis [10] observed that the increasing volume fraction of the microsphere in the microsphere epoxy resin composites improved its impact performance while decreased the fracture toughness and flexural strength. However, Wouterson et al. [11] reported the opposite testing observations, i.e., the presence of microsphere increased the fracture toughness but decreased the impact resistance capacity of syntactic foam. The strain rate effect of syntactic epoxy foam material has been investigated under ambient temperature [12-14]. The strain rate effect of expanded polystyrene foam under high temperature has been also investigated [15]. The failure strength of polyurethane foam exhibited nonlinear strain-rate dependency [16, 17]. To improve the mechanical properties, crumb rubber has been added into syntactic foam [18-20]. The rubber can enhance impact energy absorption through elastic deformation of rubber and preventing micro-cracks from developing into macro-cracks. It is noted that replacing the microspheres by the crumb rubber can increase the energy absorption capacity but slightly decrease the compressive strength [21]. Bagheri and Pearson [21] found that using 10% of crumb rubber is the optimal value. Further volume fraction of crumb rubber (e.g. 15%) showed a reduction in the fracture toughness. Maharsia et al. [18] found the presence of 2% rubber particles (40-75 μm) by volume quantity increased the flexural strength and energy absorption of syntactic foam. Bagheri et al. [22] conducted a critical review of the effect of crumb rubber on the fracture toughness of 2-phase syntactic foam and found that the optimal value of the crumb rubber volume fraction ranges between 10% and 20%.

The syntactic material can find applications owing to its characteristics of thermal efficiency, lightweight and high compressive strength and toughness [23, 24]. The syntactic foam material has been intensively employed for marine applications including deep-water exploration, which needs to withstand enormous water pressure while provide sufficient buoyancy [3, 25]. Sandwich structure made of two thin stiff face-sheets and various thick cores is used to absorb energy and resist loads. The cores can be made of lightweight materials such as metal foam, polymer foam and lattice materials etc. For instance, the syntactic foam material with aluminium matrix can be used as protection system in military vehicles to withstand blast and impact loads and protect the passengers [26]. The material has the potential for infrastructural protection of vehicle roadside barrier as energy absorption device, which can effectively reduce the impact force [27]. In addition, the lightweight material can be used to protect the offshore structure against ship impact and underwater impact of the pipeline caused by dropping objects. By considering its great potential for impact applications, the behaviours of syntactic foam under impact are worth studying. However, the research on the dynamic response of syntactic material subjected to impact loading is limited and some contradicted findings pertaining to the presence and volume fraction of microsphere on the mechanical properties of syntactic foam were reported.

This study experimentally investigates the behaviours of four types of syntactic materials, associated with/without crumb rubber and with (3-phase)/without (2-phase) macro-spheres, subjected to quasi-static and impact loads. The fracture toughness and static/impact energy absorption of the syntactic foams are experimentally investigated.

2. Production of the syntactic foam

2.1. Composition and properties of materials

Four types of syntactic foam are investigated in this study. They are classified into 2-phase and 3-phase syntactic foams and which are further divided into two types of white (without crumb rubber) and black (with crumb rubber) materials. The 2-phase syntactic foam includes epoxy and glass microspheres (~ 50 μm diameter) with/without crumb rubber. The syntactic foam without crumb rubber is named as white material while the one with crumb rubber is called black material. Carbon fibre reinforced macro-spheres (~ 10 mm diameter) were added to the 2-phase syntactic foam to form 3-phase syntactic foam.

The carbon fibre reinforced macro-spheres had the diameter of 10 mm as presented in Fig. 1. The macro-spheres were coated with carbon fibre to significantly improve their compressive strength. The macro-sphere production is usually a commercial secret of a marine equipment production company. The epoxy and glass microspheres were supplied by Matrix [28]. The glass microspheres appear as free flowing white powder to naked eyes. They were made of Borosilicate glass with the density ranging from 100 kg/m^3 to over 1000 kg/m^3. The average diameter of the glass microspheres is approximately 50 μm. The crumb rubber was produced from recycled car tyres so that it was a mixture of different blends of rubbers and fillers. A laser diffraction particle size test was conducted on the crumb rubber according to ISO 13320 [29]. The distribution of crumb rubber particle size is presented in Fig. 2. The composition of these component materials is presented in Table 1. The volume fraction of the crumb rubber of 15% was decided after conducting a review of its optimal value as presented in the previous study [22]. The compressive strength and modulus of the Matrix epoxy were 100 MPa and 2750 MPa, respectively. The density of the white and black 2-phase syntactic foam was 770 and 920 kg/m^3, respectively.

2.2. Production of samples

The production of the 2-phase syntactic foam is well presented in the previous study [22] so that this section does not repeat the production process and only describes the procedure of manufacturing the 3-phase syntactic foam. The required amount of carbon fibre reinforced macro-spheres (60% packing density) was put into a steel mould with the size of 100 mm x 200 mm. It is noted that a random packing of spheres is based on the previous study by He et al. [30]. If the close random packing is applied for equal particles, the packing density approaches 63% [30]. Due to a high surface-area-to-volume ratio of these specimens, the packing density in this study was approximately 60%. The mixture of the binder was prepared from the Matrix epoxy blend and Matrix glass microspheres with/without crumb rubber. There were two types of the binder used in this study, including the white and black binders. The black binder contained crumb rubber while the white binder did not. The binder was then injected into the mould in a vacuum condition. The mixture was cured at 80°C overnight, followed by a post cure at 130°C for 2 hours. The production process of the samples is presented in Fig. 3. The density of the 3-phase syntactic foam for the black and white specimens was approximately 501 kg/m^3 and 419 kg/m^3, respectively.

2.3. Microstructure

To check the syntactic foam structure, two different techniques were carried out, which included a Nikon SMZ800 stereomicroscope with a Schott KL1500LCD light source and scanning electron microscope (SEM). The Toupcam UCMOS 14000KPA digital camera associated with ToupView 3.7 software was used to capture the images. The microstructure of the 2-phase syntactic foam is presented in Fig. 4. There was only micro-sphere particles in the white specimen as shown in the left picture. Meanwhile, there were two types of particles in the black material including glass micro-spheres and rubbers as shown in the right picture. The twinkling particles represent glass micro-spheres and the grey particles stand for crumb rubber. The composition of the particles and the even distribution of the crumb rubber and other particles are shown in Fig. 4. The bonding between particles and binder plays an essential role in the structural performance of the material. Thus, the rough surface of the macro-sphere is to increase the bonding between the binder and the macro-spheres as shown in Fig. 5. The roughness of the surface is found to be significant for improving the bonding between binder and particles [8, 31, 32]. The interface bonding between the macro-spheres and the binder is examined after tests and presented in the later part.

3. Fracture Toughness Testing

3.1. Specimens and testing apparatus

The fracture toughness tests were conducted on the 2-phase syntactic foam including white (without crumb rubber) and black (with crumb rubber) materials. Two slabs were prepared using a PTFE lined steel mould with dimension of 300 mm long x 200 mm wide x 45 mm deep. Ten notched beams were prepared for each type of material as presented in Fig. 6. Each face of the specimens was milled square and parallel to create 20 mm x 40 mm x 180 mm cuboids, followed by a second milling process to form the slot. The apparatus and testing procedure comply with ASTM D5045 [33]. All specimens were stored in the laboratory to equilibrate to standard laboratory conditions for at least 3 weeks. Immediately prior to testing, a final “sharp” crack was formed at the tip of the slot by resting the cutting edge of a “box cutter” knife along the length of the slot and applying a moderate pressure by hand. It is noted that there was no cutting or scoring motions were applied. An indentation test was carried out for each material to identify the compliance of the test apparatus and the proportion of the strain energy developed in each test that could be attributed to the indentation by the rollers.

3.2. Results and discussions

The experimental results from the fracture toughness tests are respectively presented in Tables 2 and 3 for the white and black materials, respectively. It is noted that the energy correction due to the indentation of the rollers was measured as 0.019 and 0.034 J for the white and black materials, respectively. In general, the specimens failed at a cross head deflection of 0.75 mm with the loading rate of 10 mm/min [33]. To ensure the validity of the tests, the size of the specimen is chosen so that the yield stress must be greater than the minimum yield stress.

$$\begin{aligned} \sigma_{\min} = K_{Ic}\sqrt{\frac{2.5}{W-a}} &= 9.7\,MPa \quad \textit{for white material} \\ &= 10.4\,MPa \quad \textit{for black material} \end{aligned} \tag{1}$$

where σ_{min} is the minimum yield stress, K_{Ic} is the plane-strain fracture toughness, and W and a are the dimensions of the specimen presented in Fig. 6. The fracture toughness or critical stress intensity factor (K_{Ic}) and the critical strain energy release rate (G_{Ic}) are determined as follows [33]:

$$K_{Ic} = \frac{P_Q}{B\sqrt{W}} f(x) \tag{2}$$

$$G_{Ic} = \frac{U}{BW\varphi} \tag{3}$$

where P_Q is the force determined based on ASTM D5045 [33], B is the thickness of the specimen shown in Fig. 6, *f(x)* is the function of the ratio between the crack length and the specimen depth, φ is the energy calibration factor, and U is the corrected energy. The corrected energy (U) results from subtracting the energy-to-peak by the energy caused by the indentation displacement.

As presented in Tables 2-3, the average critical stress intensity factors or fracture toughness (K_{Ic}) for the white and black materials are 0.864 and 0.933 MPa$\sqrt{m}$, respectively. The increase of the critical stress intensity factor of the black material was about 8% as compared to the white material. The mean values of the critical strain energy release rate (G_{Ic}) of the white and black material are 0.332 and 0.404 kJ/m^2, respectively. It results in an increase by 22% in the critical strain energy release rate of the black material as compared to the white one. As expected, replacing the microspheres by crumb rubber increases the fracture toughness and the critical strain energy release rate of the materials. The results are consistent with previous studies [2, 10].

It is worth mentioning that micro-length scale damage is more beneficial to the energy absorption than macro-length scale damage. For instance, several micro-cracks may absorb the same amount of energy as one macro-crack. The macro-crack may fragment the material while the micro-cracks may only degrade the structural capacity and modulus. Therefore, preventing the development of the micro-cracks into the macro-cracks is the key factor to improve the fracture toughness and ductility of the material. Adding crumb rubber was found to result in the crack bridging phenomenon which improves the fracture toughness [18]. However, the increase of the fracture toughness in this study is not significant. As presented in the study by Bagheri et al. [22], the optimal volume fraction of crumb rubber needs to be identified and the authors recommended the searching range was from 10% to 20% of the volume fraction. More trial fracture toughness tests should be conducted to determine the optimal value of the volume fraction of the crumb rubber suggested between 10% and 15%.

In addition, there are many uncertainties introduced in this procedure so that it needs to be verified. ASTM D5045 [33] recommended the value of $E/(1-\nu^2)$ derived by two different methods can be cross checked:

$$\frac{E}{(1-\nu^2)} = \frac{K_{Ic}^2}{G_{Ic}} \tag{4}$$

$$\frac{E}{(1-\nu^2)} = \frac{\psi}{B(C_Q - C_i)} \tag{5}$$

where ν and E are the Poisson's ratio and tensile modulus of the material, respectively; C_Q and C_i are the compliance from the fracture tests and the indentation test, respectively; and Ψ is the calibration factor. As recommended by ASTM D5045 [33], the value estimated from Eq. 4 should be larger, and the difference is recommended to be less than 15%. As calculated, the differences determined by two different methods are 7.6% and 16.7% for the white and black materials, respectively.

The findings in this study are consistent with those from the previous study [18]. Maharsia et al. [18] observed that there was no significant difference in the modulus and stiffness of the rubberized syntactic foam (adding 2% crumb rubber) and the plain syntactic foam. The authors found an approximately 18% increase in the fracture strain with the addition of crumb rubber.

4. Compressive behaviour under quasi-static loads

The 3-phase syntactic foam was created to have light weight and relatively high strength and energy absorption capacity, thus, its compressive behaviour under static and impact loads was investigated. The Baldwin machine with the capacity of 600 kN was used to carry out the compression tests on the 3-phase syntactic foam. The loading rate was maintained at 0.5 mm/min until the specimens failed. The loading rate was carried out to comply with AS 1012.9 [34] for compressive strength tests. The specimens were machined at two ends to ensure full contact between the loading heads and the specimens. The cylindrical specimens were 100 mm in diameter and 200 mm in height. The applied load and displacement of the specimens were measured by the embedded load cell and linear variable differential transformer in the machine.

The tested specimens failed by some major cracks as presented in Fig. 7. The arbitrary failure surface of the tested specimens was observed rather than an approximately typical 45° failure surface in normal concrete. This figure shows the failure surfaces intersected carbon fiber reinforced macro-spheres. Failure of the interface between the binder and the macro-spheres was found at only one macro-sphere. In general, the interface bonding was sufficient. All the macro-spheres in the failure surface were damaged. As a result, the failure of the macro-spheres also governs the failure of the specimens. This failure mode was also observed in the previous study [3]. Since the binder and the macro-sphere govern the failure, adding crumb rubber in the binder, which is not a huge volume fraction, may not considerably affect the strength and energy absorption of the material. As a result, the behaviour of the white and black materials did not show a significant difference.

The stress-strain curves of the tested cylinders are presented in Fig. 8. The stress-strain curves of the syntactic foam increase linearly up to about 12 MPa with the corresponding strain of 1.7% The stress-strain curves of the tested specimens dropped along with the specimens failure, showing a very brittle manner , which is different from those reported by Wu et al. [3]. The 3-phase syntactic foam in the study by Wu et al. [3] failed in a more ductile manner, where the specimens reached the maximum stress at the strain of 5% and then the stress significantly dropped. As shown in Fig. 8, the slope of these curves started to decrease after reaching 12 MPa and the white and black specimens reached the maximum stresses of 16.5 and 15.5 MPa, respectively. Adding crumb rubber led to 6% reduction in the compressive strength of the rubberized syntactic foam as compared to the white one. The axial strains corresponding to the maximum stresses of the white and black specimens were 2.9% and 3.1%, respectively. The energy absorption, defined by the area under the force-displacement curves of the two specimens are 0.37 and 0.39 kN·m for the white and black materials, respectively. The energy absorption of the black specimen was about 5.4% higher than that of the white material. The two specimens did not show a considerable difference in the static behaviour. It shows that replacing 15% volume fraction of the glass microspheres by the crumb rubber does not significantly change the static behaviour of the specimens. The elastic modulus of the syntactic foam for the white and black specimens is 748 and 627 MPa, respectively.

In addition, the microstructure of the material was examined after the compression tests and presented in Fig. 9. Observation of cracks in the black material specimens was difficult so that cracks in the white material specimen are presented herein. Two types of damage modes were found in the specimen. A separation at the interface between the binder and the macro-sphere is presented in Fig. 9a. This crack is connected with another one cutting through the binder as shown in Fig. 9b. The crack in the binder shows both damages of the epoxy resin and glass micro-sphere. The crack in the binder was stopped at the macro-sphere. The failure mechanism helps to improve the ductility and thus the energy absorption performance, which demonstrated the effectiveness of coating macro-spheres. This mechanism was also observed in the previous study for micro-spheres [20].

5. Compressive behaviour under impact loads

5.1. Test setup and data acquisition system

The impact testing apparatus as shown in Fig. 10 was used to carry out drop-weight impact tests. A cylindrical steel projectile weighing 97.5 kg was dropped from 3 m height onto the top of the tested cylinders. This drop generated a kinetic energy of 2.87 kJ. The projectile was designed to have a smooth flat bottom with a radius r = 50 mm. A plastic guiding tube was utilized to ensure the projectile falling vertically to the targets. A load cell was placed at the bottom of the specimens to measure the impact force. A high-speed camera which was set to capture 20000 frames per second was used to monitor the failure process. The data acquisition system controlled by a computer was used to record signals from the load cell. The data acquisition system recorded data at a sampling rate of 1 MHz. This sampling rate was adopted according to the recommendation from a previous study [35]. Pham and Hao [35] investigated the sampling rate on the results of the axial impact tests. The authors recommended that the sampling rate smaller than 100 kHz may not be able to capture peak impact load and responses.

5.2. Test results and discussions

The high speed camera was used to monitor the failure while the image analysis was utilized to derive the displacement of the specimens. The both white and black cylinders failed in an explosive manner when the top half of the specimens was smashed. This failure mode is different from that of concrete cylinders in which the splitting failure was observed [35] (see Fig. 11). This is because the tensile properties of the syntactic foam are governed by the epoxy resin which has much higher tensile strength than that of concrete. As a result, the syntactic foam failed by crushing of the compressive material rather than splitting as in concrete. The progressive failure of the white specimen is shown in Fig. 12. Spalling of the white syntactic foam at the top started at about 0.8 ms after the impact. A vertical crack initiated at the impacted end propagated downward and became visible at 1 ms. The white specimen was severely smashed in a very brittle manner at 2.35 ms. Meanwhile, the black specimen did not exhibit damage up to 1 ms after the impact. At 1.45 ms, the black specimen showed significant damage in the top half. The failure modes of the two specimens showed similar manner, which indicates using 15% volume fraction crumb rubber did not considerably reduce the brittleness of the material.

The impact force time histories of the two specimens are presented in Figs. 13-14. During the impact event, the projectile may impact the specimens one or multiple times depending on the projectile-specimen interaction. It is noted that the time scale of the impact force measured by a load cell and those from the high speed camera are not synchronized. For the white specimen, the projectile first impacted the specimen so that the projectile and the top surface of the specimen moved with two different velocities in the same direction. They then lost contact in a very short period of approximate 35 ms before being in contact again as shown in Fig. 13. The impact force of the white specimen reached the maximum value at the second peak of 372 kN. The impulses of the first and second impacts of the white specimen are 136 and 602 kN·ms, respectively. The duration of the first and the second impacts of the white specimen was 1 ms and 5 ms, respectively. The impact force of the black specimen reached the peak of 231 kN with the corresponding duration of 1 ms, resulting in the impulse of 138 kN·ms (Table 4). It can be concluded that the white material can withstand higher impact force and impulse than the black material. The impulse of the impact force is defined as a measure of the impact resistance capacity of the tested specimens. The replacement of glass microsphere by crumb rubber decreased the impact impulse capacity of syntactic foam.

In this study, the impact energy absorption is estimated based on the energy conservation law in which the impact velocity and the residual velocity of the projectile were traced from the image processing technique. As shown in Fig. 15, the two specimens had similar impact velocities (6.76 m/s) but the black specimen exhibited a lower residual velocity than that of the white specimen (5.96 m/s vs 6.33 m/s). As a result, the black specimen absorbed 1136 J while the energy absorption of the while specimen was 915 J as shown in Fig. 16. The impact energy absorption of the material was about 3 times its energy absorption under static loads as shown in Table 4. In this study, replacing glass microspheres by crumb rubber leads to 24% increase of the impact energy absorption while the energy absorption enhancement under static load was only 5%. This increase agrees with the testing results by Li and John [20] in which they found that rubberized syntactic foam with 20% volume fraction had a higher capacity to absorb impact energy and resist bending strength via the positive composite action between glass microsphere and crumb rubber. The co-existence of stiff particles (i.e. glass microsphere) and soft particles (i.e. crumb rubber) can adjust and reduce stress concentration. As reported, the initiation energy (i.e. elastic strain energy absorption) increased by replacing a portion of glass microspheres by crumb rubber, which proved the positive effect of adding crumb rubber.

In addition, the specific energy absorption of these specimens were observed as 583 kJ/m^3 for the white foam and 723 kJ/m^3 for the black foam. The specific energy of the syntactic foam in this study was about 10 times smaller than that of the hollow glass microsphere/epoxy based syntactic foam (6-15 MJ/m^3) reported by Swetha and Kumar [2]. This difference is reasonable since the compressive strength of the syntactic foam in the study by Swetha and Kumar [2] was approximately 6 times stronger than that of the syntactic foam in this study. Meanwhile, Walter et al. [36] reported the similar energy absorption of epoxy-based syntactic foam ranging from 200 – 2000 kJ/m^3 when materials with similar strength were used. Therefore, the glass microspheres partially replaced by the crumb rubber yielded higher energy absorption but lower impact impulse capacity. Adding crumb rubber to the syntactic foam can increase the energy absorption but reduce the compressive strength of the material. This may be due to the fact that at a high volume fraction of crumb rubber, not much epoxy is available for bonding the matrix and transferring stresses prior to fracture. In addition to examine the dynamic increase factor, the compressive stresses of the specimens are presented in Figs. 17-18. As shown in these figures, the material is strain rate sensitive as the compressive stress of these specimens was approximately double their static strengths. This increase reasonably agrees with the experimental results reported by Zhang et al. [6] in which split Hopkinson pressure bar was used to investigate the dynamic properties of syntactic foam with hollow glass spheres. The authors observed the dynamic increase factor from 1.2 to 2.2 in varied strain rates from $0.01 s^{-1}$ to $2750 s^{-1}$. It is noted that accurate strain measure could not be achieved with the drop-weight tests so that better equipment (e.g. split Hopkinson pressure bar) should be used to further investigate the strain rate effect on the mechanical properties of the syntactic foam.

5.3. Microstructure investigation

Unlike the specimens under the static tests, macro-spheres coated by fibre became brittle under impact loads, which was also observed in the previous study [35]. Pham and Hao [35] presented that carbon and glass fibre show very brittle behaviour under impact loads, and glass fibre performs much better than carbon fibre due to its high rupture strain. Fig. 19 shows the failure of the white specimen at the interface and a macro-sphere while this failure was not seen in the rubberized specimen. The macro-sphere was broken in the plane at an angle to the failure surface during the impact event, indicating the brittleness of macro-spheres. This failure indicates the white binder can transfer a sufficiently higher stress to a macro-sphere as compared to the black binder. It is noted that the coated macro-spheres for the rubberized specimen did not show damage in the angled plane respect to the failure surface. In general, adding crumb rubber did not show a significant difference of the material properties under static loads but it resulted in a considerable change under impact loads as shown in Figs. 13-14, indicating it is sensitive to impact loads. This phenomenon also indicates that the white specimen is able to absorb more energy than the rubberized specimen due to more damage occurred in macro-spheres as evident in the impact tests.

In addition, the quality of the bonding between crumb rubbers and the epoxy is very important to the material performance. Kaynak et al. [37] observed poor bonding and separation between the crumb rubbers from waste tyres while Maharsia et al. [18] found a good bonding between the crumb rubbers and the epoxy. A sound bonding between the crumb rubber and epoxy was found in this study.

6. Conclusions

Replacing 15% volume fraction of the glass microsphere by the crumb rubber slightly increases energy absorption capacity of the syntactic foam under quasi-static loads but not impact loads. The density of the 3-phase syntactic foam is about 25% of that of normal strength concrete but it has a similar fracture toughness.

For the 2-phase syntactic foam, introducing 15% volume fraction of the crumb rubber slightly increases the fracture toughness (8%) and the fracture energy (22%). More trial fracture toughness tests should be conducted to determine the optimal value of the volume fraction of the crumb rubber between 10% and 15%.

For the 3-phase syntactic foam under quasi-static loads, the compressive strength and elastic modulus of the rubberized syntactic foam reduces by 6% and 16.1%, respectively. The energy absorption capacity of the black material increases by 5.1% as compared to the white material. The volume fraction of the crumb rubber is recommended to be reduced for a better performance on the energy absorption of the 3-phase syntactic foam.

The impact impulse resistance of the 3-phase rubberized syntactic foam is inferior as compared to the 3-phase syntactic foam without crumb rubber. However, the impact energy absorption of the 3-phase rubberized syntactic foam increased by 24% as compared to that of the syntactic foam without crumb rubber.

In summary, the optimal volume fraction of crumb rubber may fall between 10% and 15%. When 3-phase syntactic foam is introduced, it should have lower volume fraction of crumb rubber as compared to that in 2-phase syntactic foam. The optimal values depend on 2-phase or 3-phase syntactic foam and static or dynamic loading conditions.

Acknowledgement

The support from Australian Research Council via Discovery Early Career Researcher Award (DE160101116) is acknowledged.

References

[1] Shutov FA. Syntactic polymer foams. Chromatography/Foams/Copolymers: Springer; 1986. p. 63-123.

[2] Swetha C, Kumar R. Quasi-static uni-axial compression behaviour of hollow glass microspheres/epoxy based syntactic foams. Materials & Design. 2011;32(8-9):4152-63.

[3] Wu X, Dong L, Zhang F, Zhou Y, Wang L, Wang D, Yin Y. Preparation and characterization of three phase epoxy syntactic foam filled with carbon fiber reinforced hollow epoxy macrospheres and hollow glass microspheres. Polym Compos. 2016;37(2):497-502.

[4] Narkis M, Kenig S, Puterman M. 3-Phase syntactic foams. Polym Compos. 1984;5(2):159-65.

[5] Lapčík L, Ruszala MJA, Vašina M, Lapčíková B, Vlček J, Rowson NA, Grover LM, Greenwood RW. Hollow spheres as nanocomposite fillers for aerospace and automotive composite materials applications. Composites Part B: Engineering. 2016;106:74-80.

[6] Zhang X, Wang P, Zhou Y, Li X, Yang E-H, Yu TX, Yang J. The effect of strain rate and filler volume fraction on the mechanical properties of hollow glass microsphere modified polymer. Composites Part B: Engineering. 2016;101:53-63.

[7] Gupta N, Ye R, Porfiri M. Comparison of tensile and compressive characteristics of vinyl ester/glass microballoon syntactic foams. Composites Part B: Engineering. 2010;41(3):236-45.

[8] Huang R, Li P. Elastic behaviour and failure mechanism in epoxy syntactic foams: The effect of glass microballoon volume fractions. Composites Part B: Engineering. 2015;78:401-8.

[9] Porfiri M, Gupta N. Effect of volume fraction and wall thickness on the elastic properties of hollow particle filled composites. Composites Part B: Engineering. 2009;40(2):166-73.

[10] Kim HS, Khamis MA. Fracture and impact behaviours of hollow micro-sphere/epoxy resin composites. Composites Part A: Applied Science and Manufacturing. 2001;32(9):1311-7.

[11] Wouterson EM, Boey FYC, Hu X, Wong S-C. Fracture and Impact Toughness of Syntactic Foam. Journal of Cellular Plastics. 2004;40(2):145-54.

[12] Song B, Chen WW, Lu WY. Mechanical characterization at intermediate strain rates for rate effects on an epoxy syntactic foam. International Journal of Mechanical Sciences. 2007;49(12):1336-43.

[13] Li P, Petrinic N, Siviour CR, Froud R, Reed JM. Strain rate dependent compressive properties of glass microballoon epoxy syntactic foams. Materials Science and Engineering: A. 2009;515(1-2):19-25.

[14] Koohbor B, Mallon S, Kidane A, Lu W-Y. The deformation and failure response of closed-cell PMDI foams subjected to dynamic impact loading. Polym Test. 2015;44:112-24.

[15] Krundaeva A, De Bruyne G, Gagliardi F, Van Paepegem W. Dynamic compressive strength and crushing properties of expanded polystyrene foam for different strain rates and different temperatures. Polym Test. 2016;55(Supplement C):61-8.

[16] Whisler D, Kim H. Experimental and simulated high strain dynamic loading of polyurethane foam. Polym Test. 2015;41(Supplement C):219-30.

[17] Weißenborn O, Ebert C, Gude M. Modelling of the strain rate dependent deformation behaviour of rigid polyurethane foams. Polym Test. 2016;54(Supplement C):145-9.

[18] Maharsia R, Gupta N, Jerro HD. Investigation of flexural strength properties of rubber and nanoclay reinforced hybrid syntactic foams. Materials Science and Engineering: A. 2006;417(1-2):249-58.

[19] Li G, Jones N. Development of rubberized syntactic foam. Composites Part A: Applied Science and Manufacturing. 2007;38(6):1483-92.

[20] Li G, John M. A crumb rubber modified syntactic foam. Materials Science and Engineering: A. 2008;474(1):390-9.

[21] Bagheri R, Pearson RA. Role of particle cavitation in rubber-toughened epoxies: 1. Microvoid toughening. Polymer. 1996;37(20):4529-38.

[22] Bagheri R, Marouf B, Pearson R. Rubber-toughened epoxies: a critical review. Journal of Macromolecular Science®, Part C: Polymer Reviews. 2009;49(3):201-25.

[23] Gibson L, Ashby M. Cellular solids: structure and properties. Cambridge: Cambridge University Press; 2003.

[24] Nasim M, Brasca M, Khosroshahi SF, Galvanetto U. Understanding the impact properties of polymeric sandwich structures used for motorcyclists' back protectors. Polym Test. 2017;61(Supplement C):249-57.

[25] Le Gall M, Choqueuse D, Le Gac P-Y, Davies P, Perreux D. Novel mechanical characterization method for deep sea buoyancy material under hydrostatic pressure. Polym Test. 2014;39(Supplement C):36-44.

[26] Altenaiji M, Guan ZW, Cantwell WJ, Zhao Y, Schleyer GK. Characterisation of aluminium matrix syntactic foams under drop weight impact. Materials & Design. 2014;59:296-302.

[27] Kim HS, Oh HH. Manufacturing and impact behavior of syntactic foam. J Appl Polym Sci. 2000;76(8):1324-8.

[28] Matrix. Syntactic foam. http://www.matrixengineered.com/. Accessed on 2nd November 2017.

[29] ISO 13320. Particle Size Analysis: Laser Diffraction Methods: International Organization for Standardization; 2009.

[30] He D, Ekere N, Cai L. Computer simulation of random packing of unequal particles. Physical review E. 1999;60(6):7098.

[31] Licitra L, Luong DD, Strbik Iii OM, Gupta N. Dynamic properties of alumina hollow particle filled aluminum alloy A356 matrix syntactic foams. Materials & Design. 2015;66, Part B:504-15.

[32] Taherishargh M, Belova IV, Murch GE, Fiedler T. On the mechanical properties of heat-treated expanded perlite–aluminium syntactic foam. Materials & Design. 2014;63:375-83.

[33] ASTM D5045. Standard test methods for plane-strain fracture toughness and strain energy release rate of plastic materials. D5045:2014. West Conshohocken, PA2014.

[34] AS 1012.9. Compressive strength tests - concrete. 10129: 2014. Sydney, NSW, Australia2014.

[35] Pham TM, Hao H. Axial Impact Resistance of FRP-Confined Concrete. J Compos Constr. 2017;21(2):04016088.

[36] Walter T, Sietins J, Moy P. Evaluation of Syntactic Foam for Energy Absorption at Low to Moderate Loading Rates. Advanced Composites for Aerospace, Marine, and Land Applications II: Springer; 2015. p. 233-44.

[37] Kaynak C, Sipahi-Saglam E, Akovali G. A fractographic study on toughening of epoxy resin using ground tyre rubber. Polymer. 2001;42(9):4393-9.

List of Figures

List of Tables

Table 1. Composition of component materials

Material		Volume fraction of matrix (%)			Macro spheres (packing density)
		Epoxy blend	Glass microspheres	Crumb rubber (75 µm)	
2-phase	White syntactic foam	64	36	nil	nil
	Black syntactic foam	64	21	15	nil
3-phase	White syntactic foam	64	36	nil	60%
	Black syntactic foam	64	21	15	60%

Table 2. Experimental results of fracture toughness tests for the white material

No.	Ligament width (mm)	Width (mm)	Crack length (mm)	Peak force (N)	K_{Ic} [a] (MPa $\sqrt{m}$)	Energy to peak (Nm)	Corrected energy (Nm)	G_{Ic} [b] (kJ/m^2)
1	20.1	40.2	20.10	304	0.809	0.073	0.054	0.272
2	20.2	40.0	19.80	331	0.873	0.086	0.067	0.337
3	20.2	39.9	19.70	311	0.81	0.071	0.052	0.260
4	20.2	40.1	19.90	338	0.876	0.093	0.074	0.363
5	20.1	40.0	19.90	317	0.839	0.084	0.065	0.325
6	20.1	40.2	20.10	336	0.894	0.098	0.079	0.395
7	20.1	40.2	20.10	349	0.928	0.098	0.079	0.397
8	20.1	40.1	20.00	331	0.869	0.081	0.062	0.307
9	20.2	40.1	19.90	349	0.909	0.096	0.077	0.382
10	20.1	40.0	19.90	313	0.828	0.075	0.056	0.283
Mean		40.1	19.9	328	0.864	0.086	0.067	0.332
SD		0.1	0.14	15.9	0.041	0.010	0.010	0.051

[a] Critical stress intensity factor

[b] Critical strain energy release rate

Table 3. Experimental results of fracture toughness tests for the black material

No.	Ligament width (mm)	Width (mm)	Crack length (mm)	Peak force (N)	K_{Ic} [a] (MPa $\sqrt{m}$)	Energy to peak (Nm)	Corrected energy (Nm)	G_{Ic} [b] (kJ/m^2)
1	20.2	40.2	20.0	342	0.889	0.117	0.083	0.408
2	20.1	40.2	20.1	379	1.013	0.126	0.092	0.464
3	20.0	40.2	20.2	354	0.935	0.107	0.073	0.362
4	20.3	40.2	19.9	370	0.954	0.124	0.090	0.443
5	20.1	40.2	20.1	347	0.919	0.109	0.075	0.377
6	20.2	40.2	20.0	327	0.850	0.097	0.063	0.312
7	20.1	40.1	20.0	369	0.974	0.124	0.090	0.447
8	20.1	40.1	20.0	345	0.920	0.113	0.079	0.397
9*	20.2	40.3	20.1	362	0.944	0.122	0.088	0.432
Mean		40.2	20.0	355	0.933	0.115	0.081	0.404
SD		0.1	0.1	16.4	0.047	0.010	0.010	0.048

* Data of specimen no. 10 was lost

[a] Critical stress intensity factor

[b] Critical strain energy release rate

Table 4. Experimental results of 3-phase syntactic foam

Testing condition	Characteristic	White foam	Black foam
Static load	Compressive strength (MPa)	16.5	15.5
	Elastic modulus (MPa)	748	627
	Energy absorption (kJ)	0.37	0.39
Impact load	Peak impact force (kN)	295/372[*]	231
	Impact duration (ms)	1/5[*]	1
	Impact impulse (kN.ms)	136/602[*]	138
	Energy absorption (kJ)	0.92	1.14
	Specific energy (kJ/m^3)	583	723

[*] Results corresponding to the first and second peaks

Glass spheres (D50 μm) Carbon fiber reinforced macro-spheres (D10 mm)

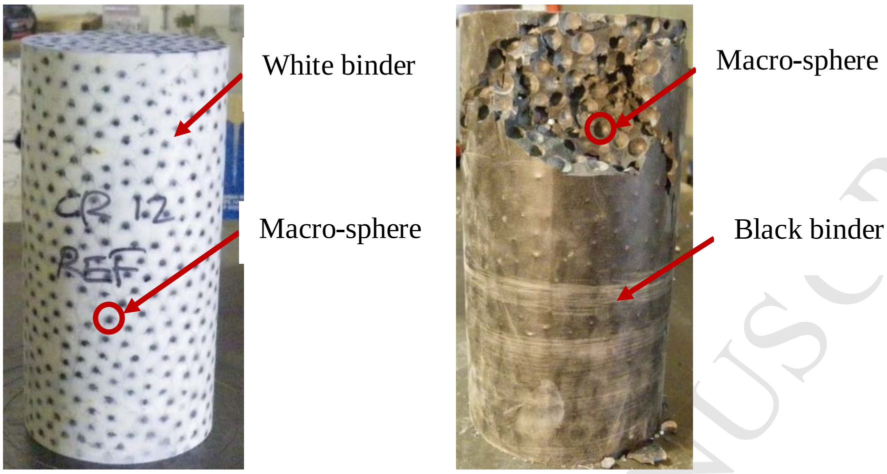

White syntactic foam Black syntactic foam

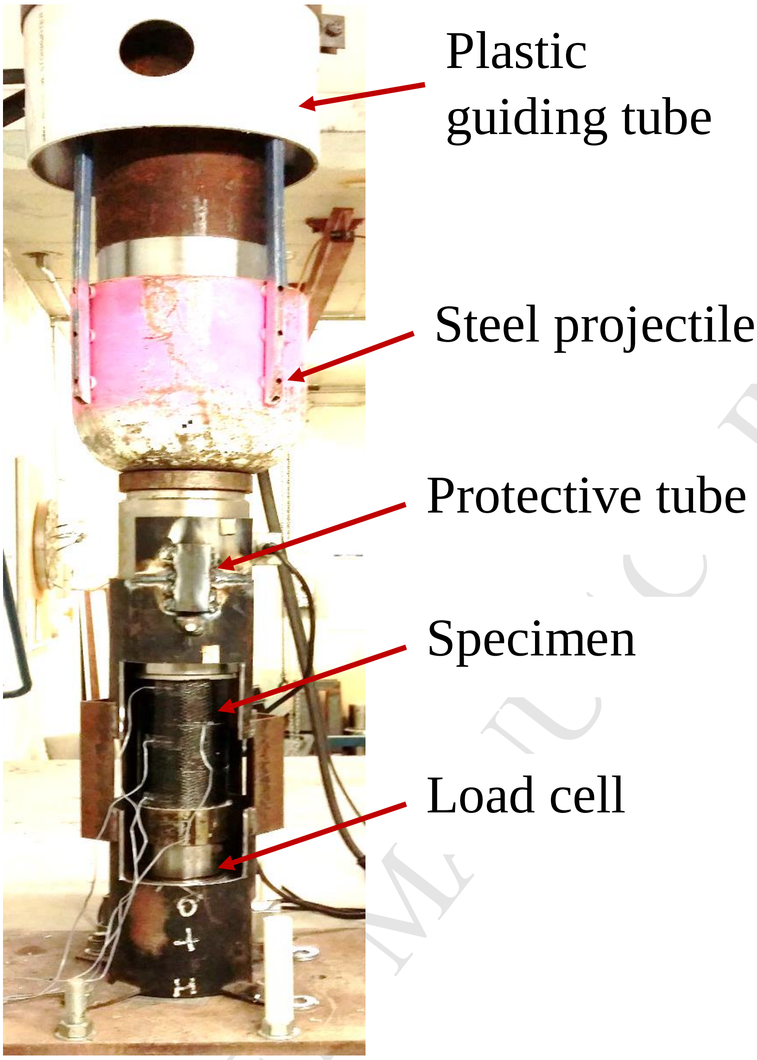
Plastic
guiding tube
Steel projectile
Protective tube
Specimen
Load cell

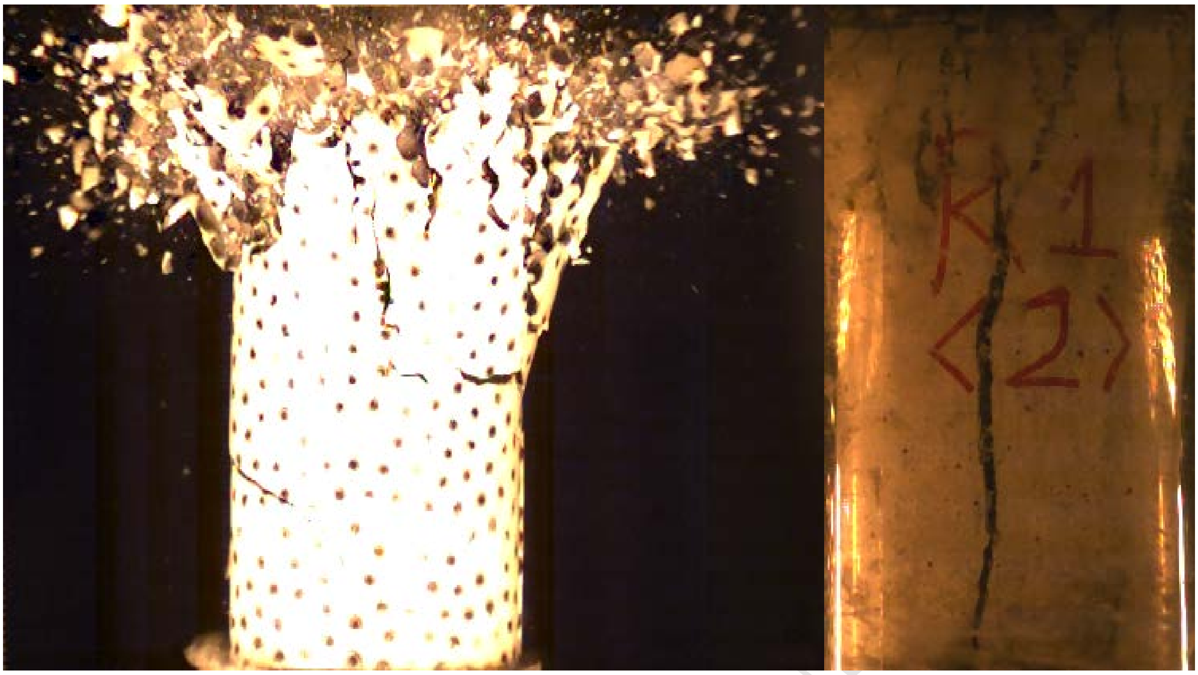

Crushing failure of syntactic foam

Splitting failure of concrete

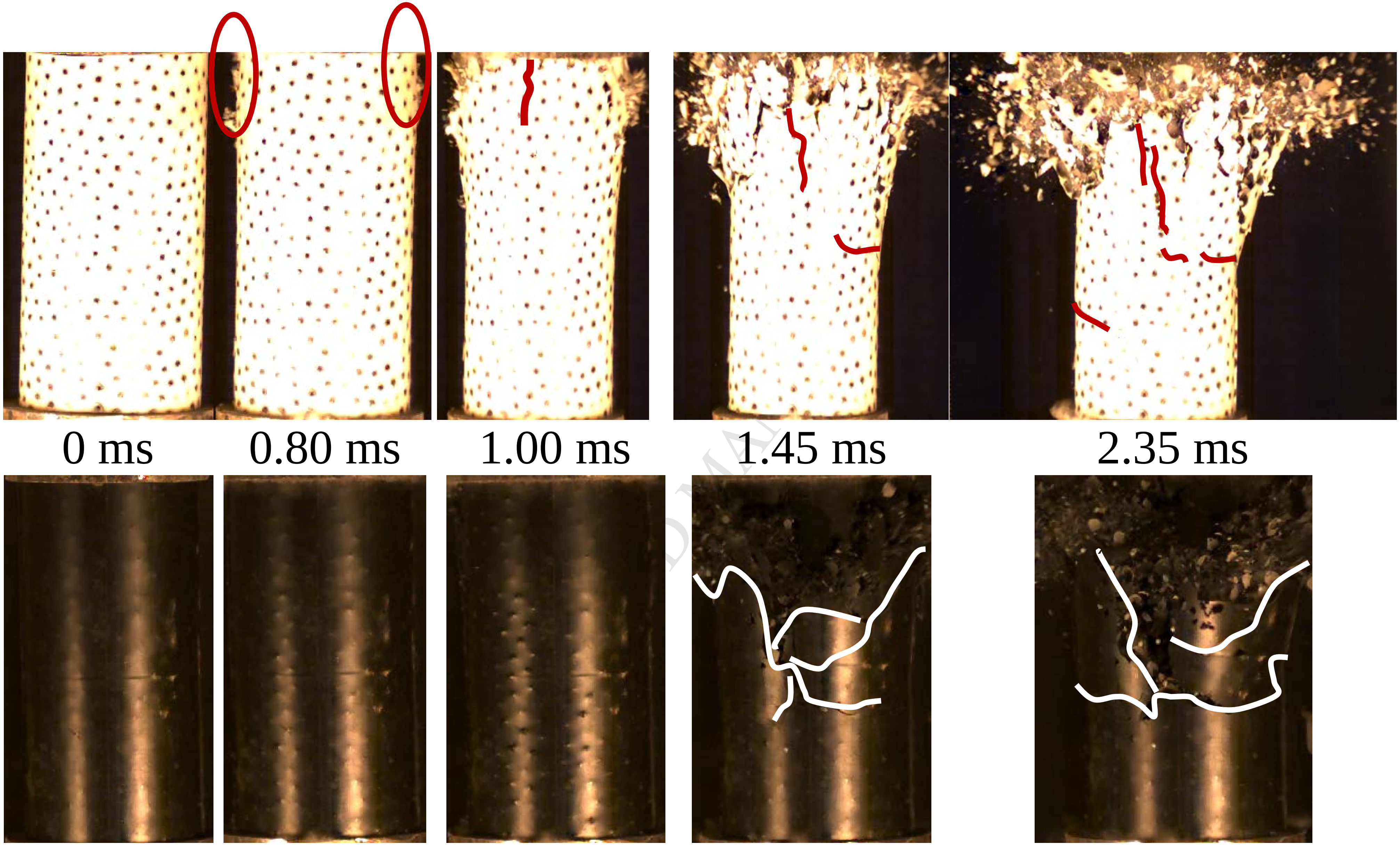
0 ms
0.80 ms
1.00 ms
1.45 ms
2.35 ms

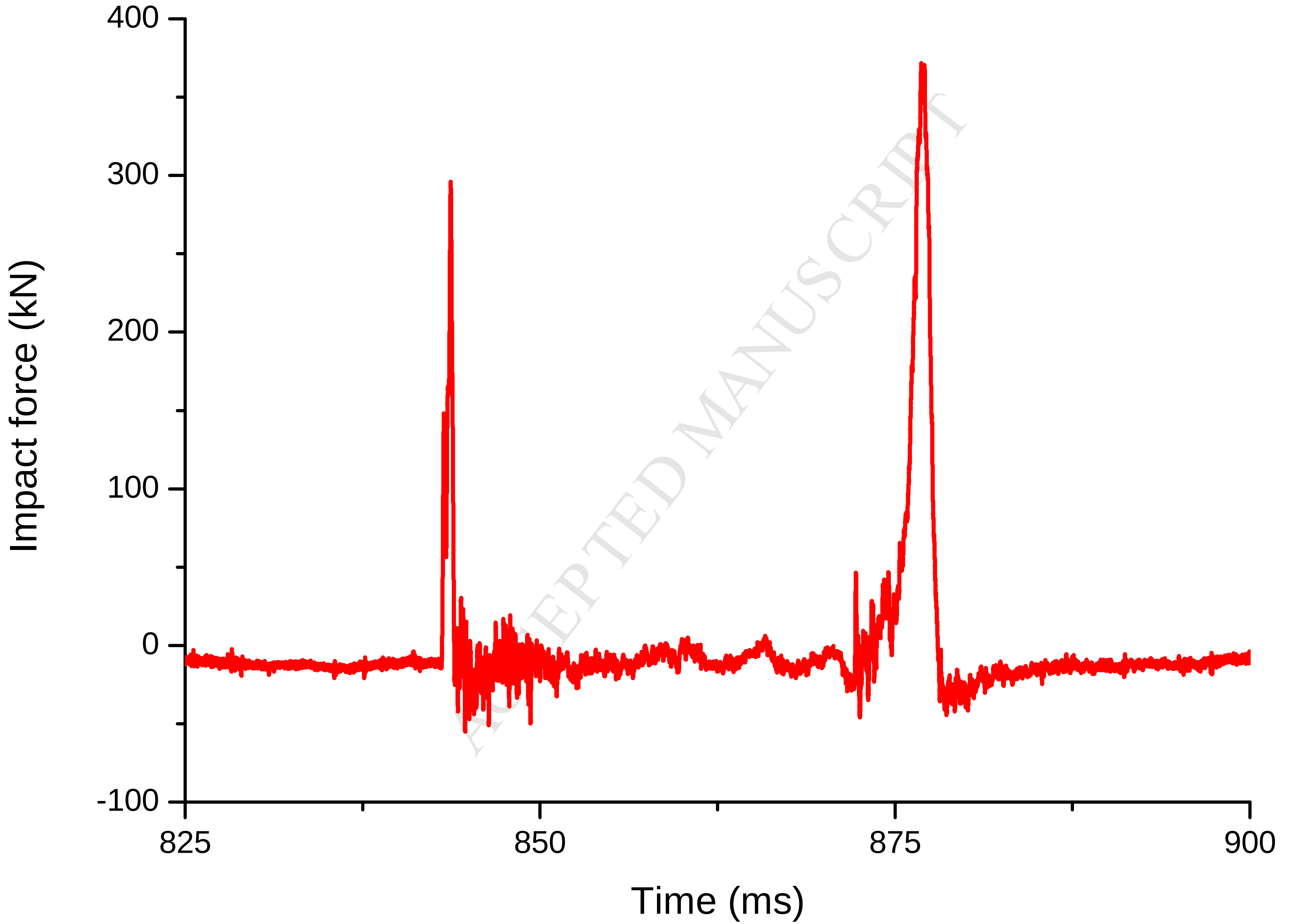
400
300
200
100
0
-100
Impact force (kN)
825
850
875
900
Time (ms)

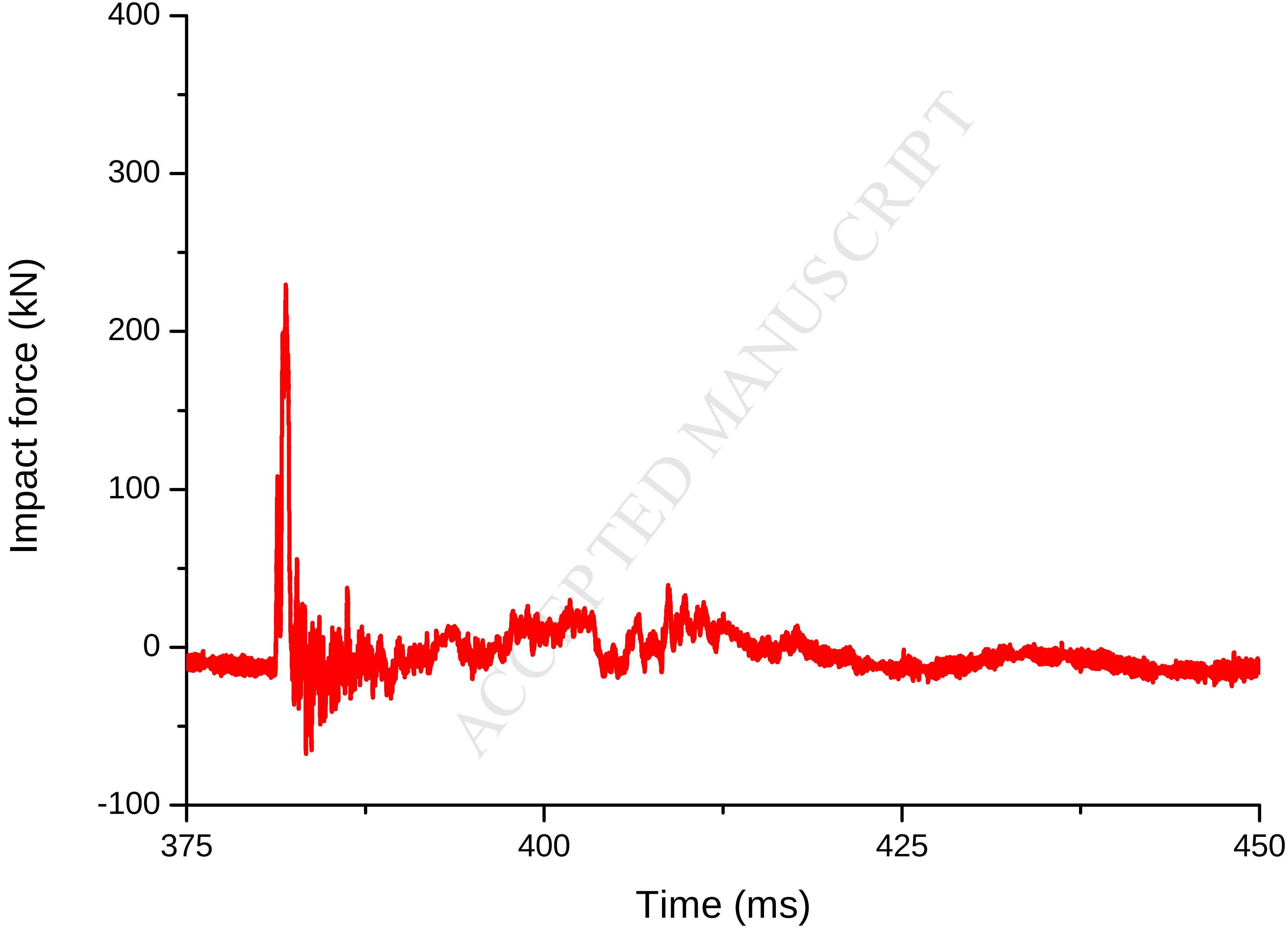
400
300
200
100
0
-100
Impact force (kN)
375
400
425
450
Time (ms)

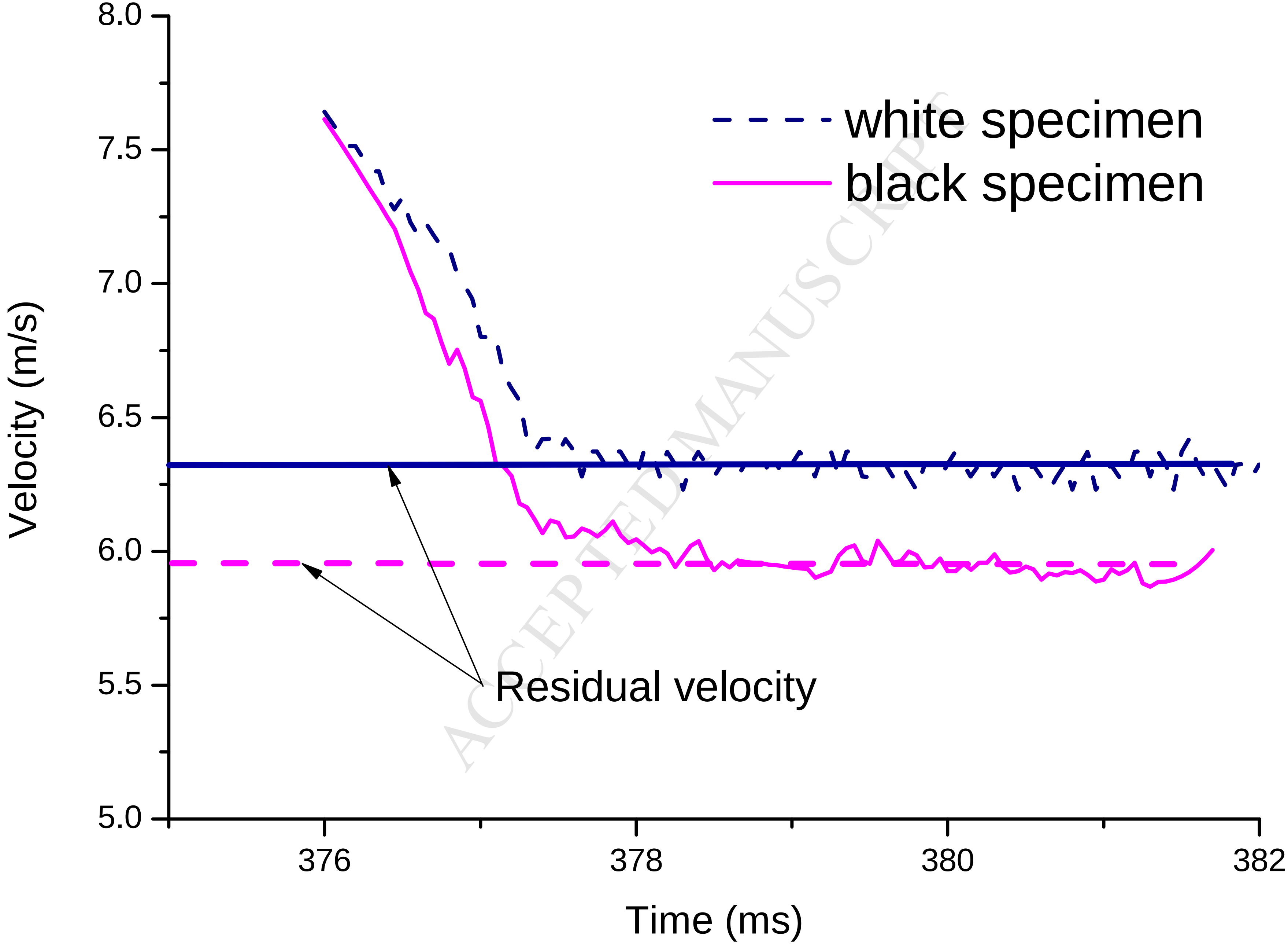

8.0
7.5
7.0
6.5
6.0
5.5
5.0
Velocity (m/s)
376
378
380
382
Time (ms)
white specimen
black specimen
Residual velocity

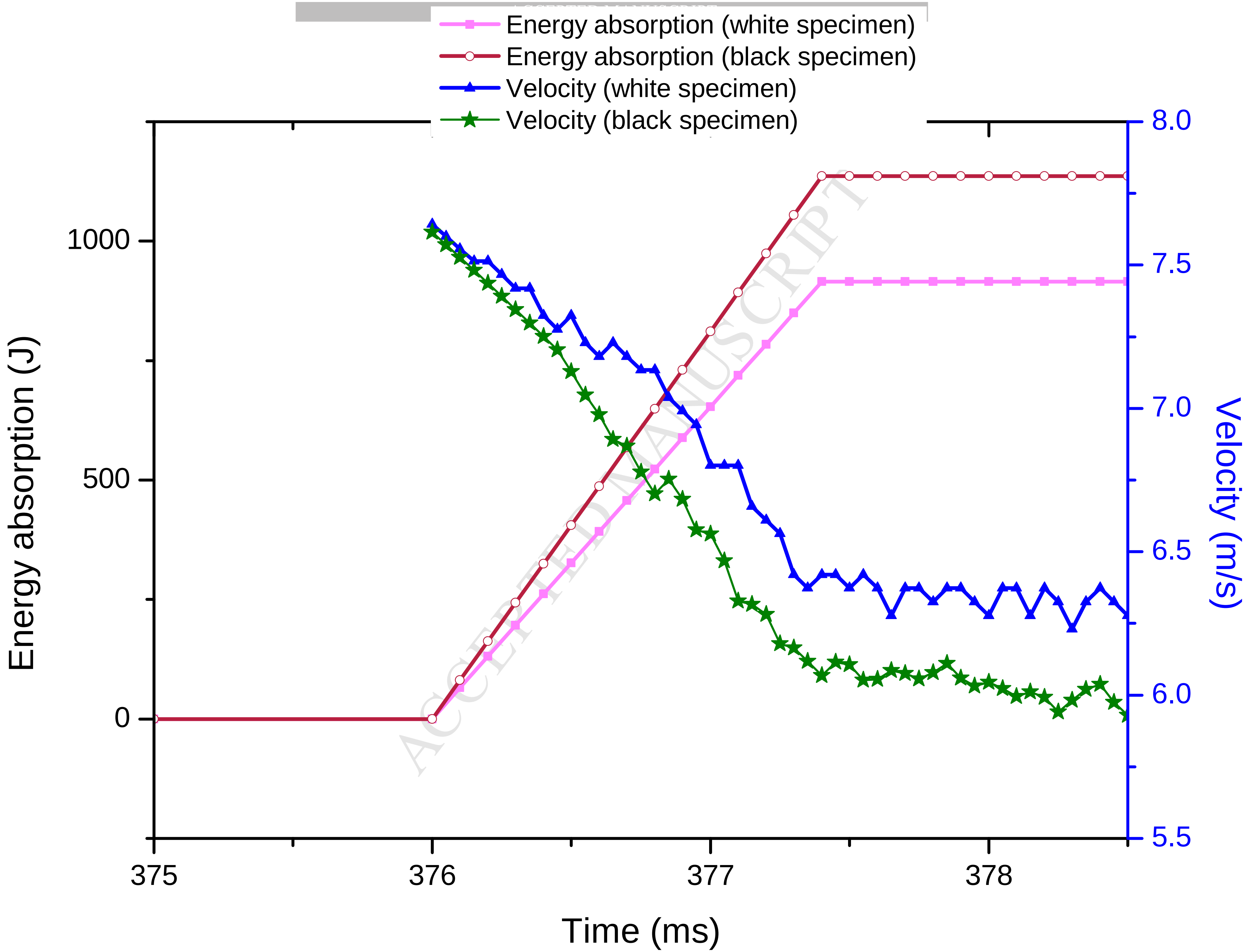

Energy absorption (white specimen)
Energy absorption (black specimen)
Velocity (white specimen)
Velocity (black specimen)
Energy absorption (J)
0
500
1000
Velocity (m/s)
5.5
6.0
6.5
7.0
7.5
8.0
Time (ms)
375
376
377
378

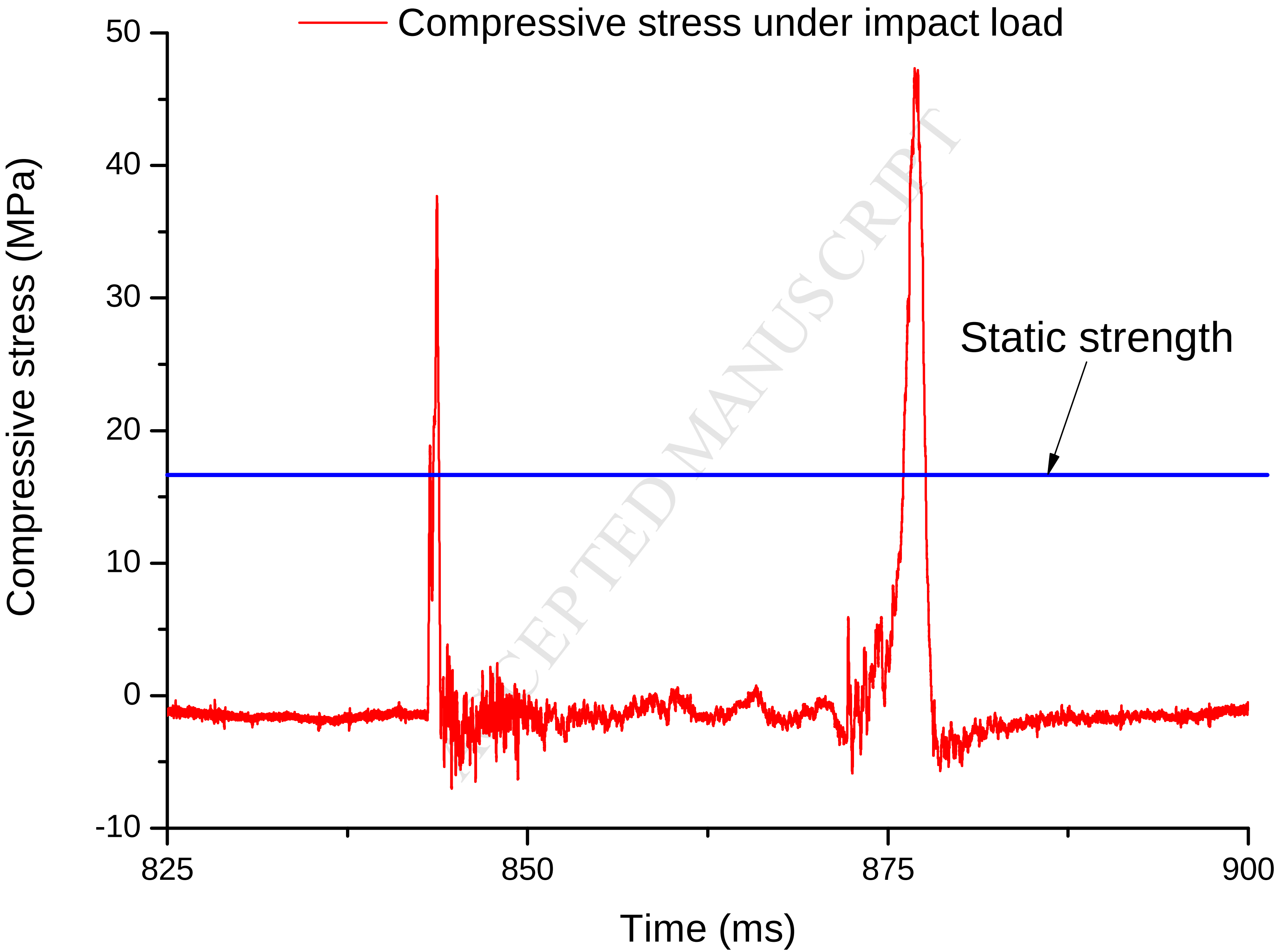
Compressive stress under impact load
Static strength
Compressive stress (MPa)
Time (ms)
50
40
30
20
10
0
-10
825
850
875
900

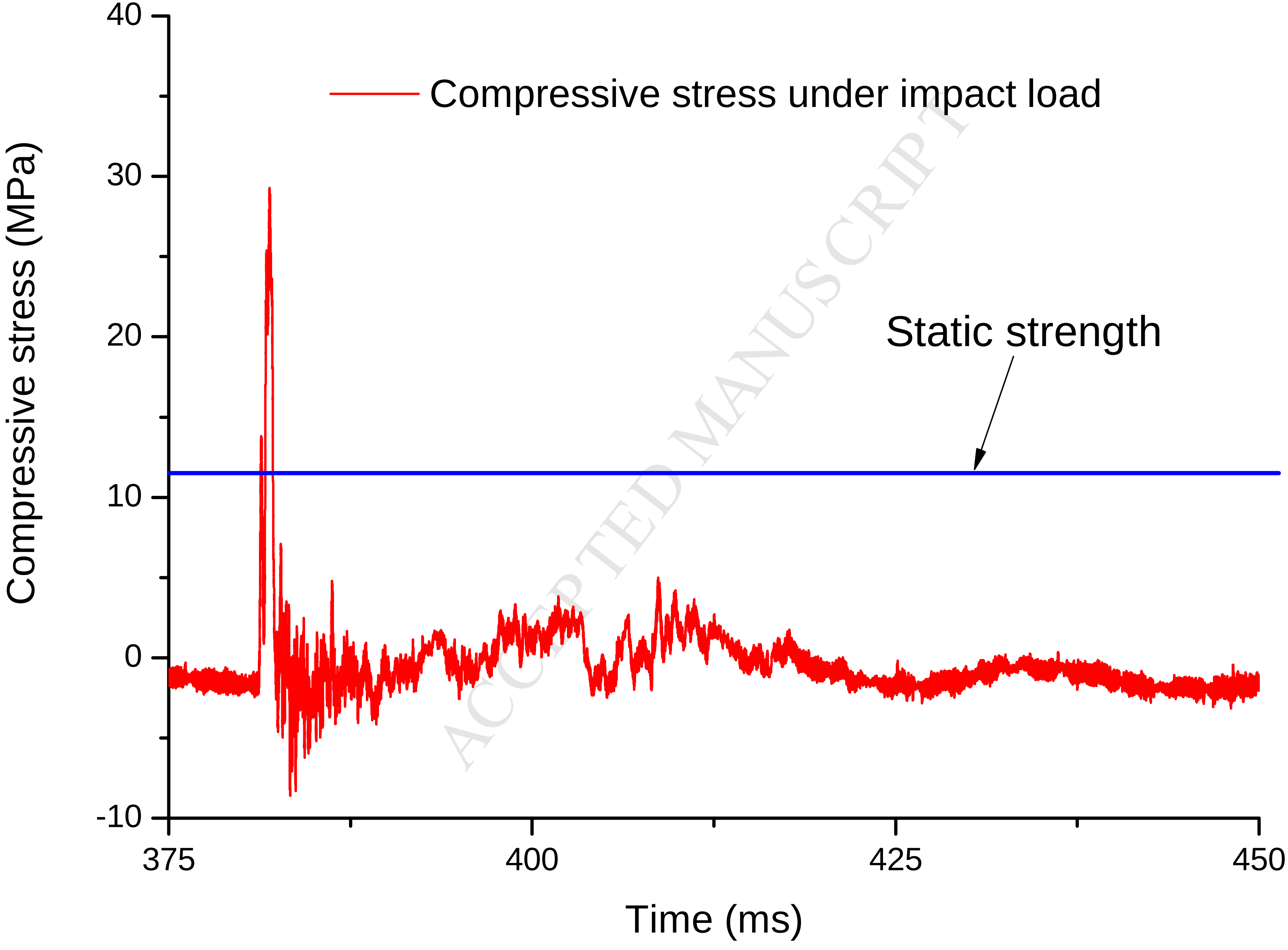
Compressive stress under impact load
Static strength
Compressive stress (MPa)
Time (ms)
40
30
20
10
0
-10
375
400
425
450

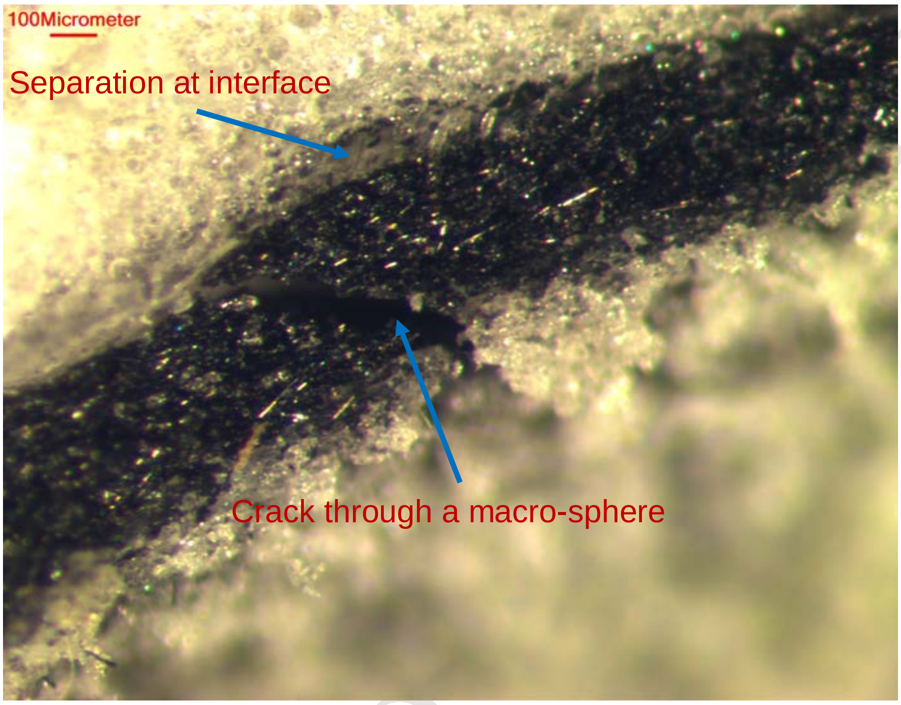
100Micrometer
Separation at interface
Crack through a macro-sphere

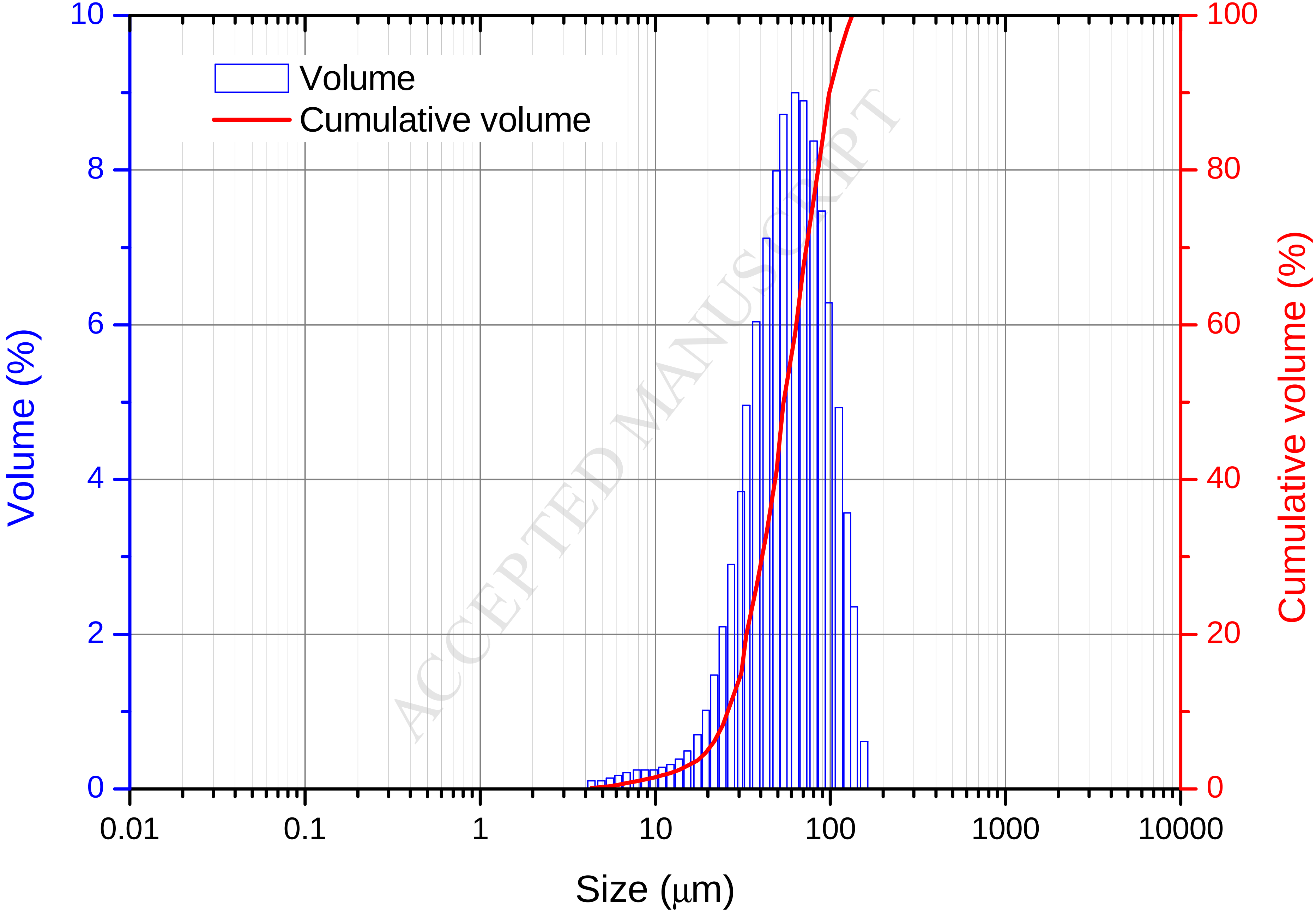
Volume
Cumulative volume
Volume (%)
Cumulative volume (%)
Size (μm)
0
2
4
6
8
10
0
20
40
60
80
100
0.01
0.1
1
10
100
1000
10000

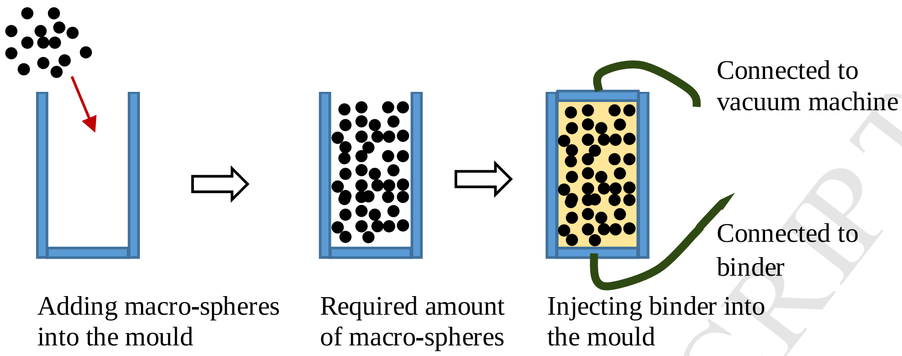

Connected to
vacuum machine
Connected to
binder
Adding macro-spheres
into the mould
Required amount
of macro-spheres
Injecting binder into
the mould

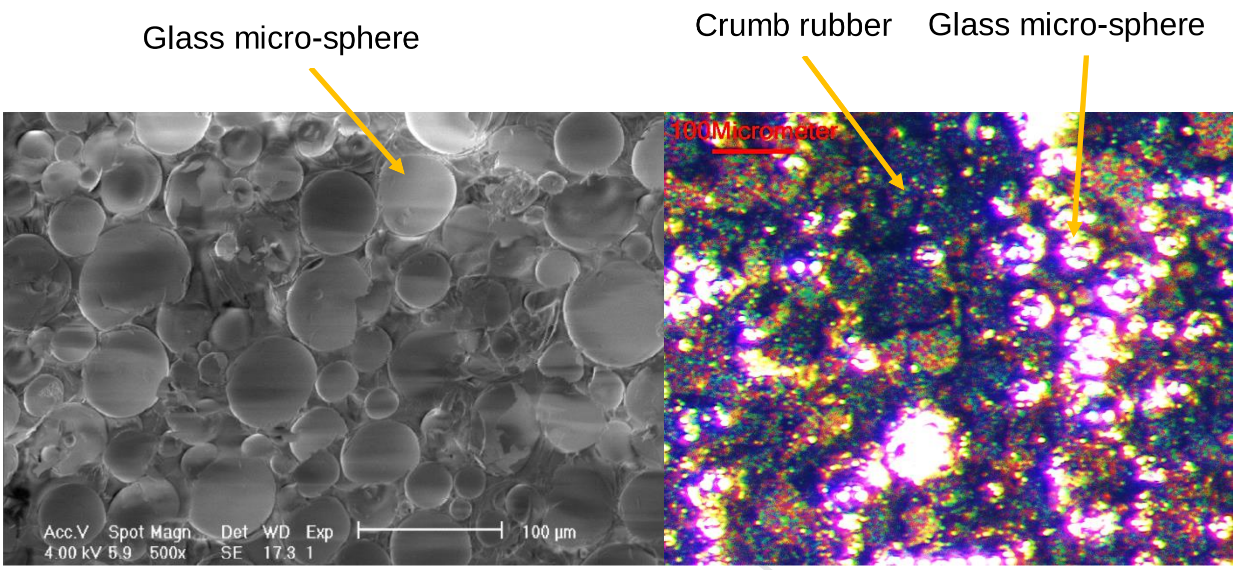

Syntactic foam without crumb rubber Syntactic foam with crumb rubber

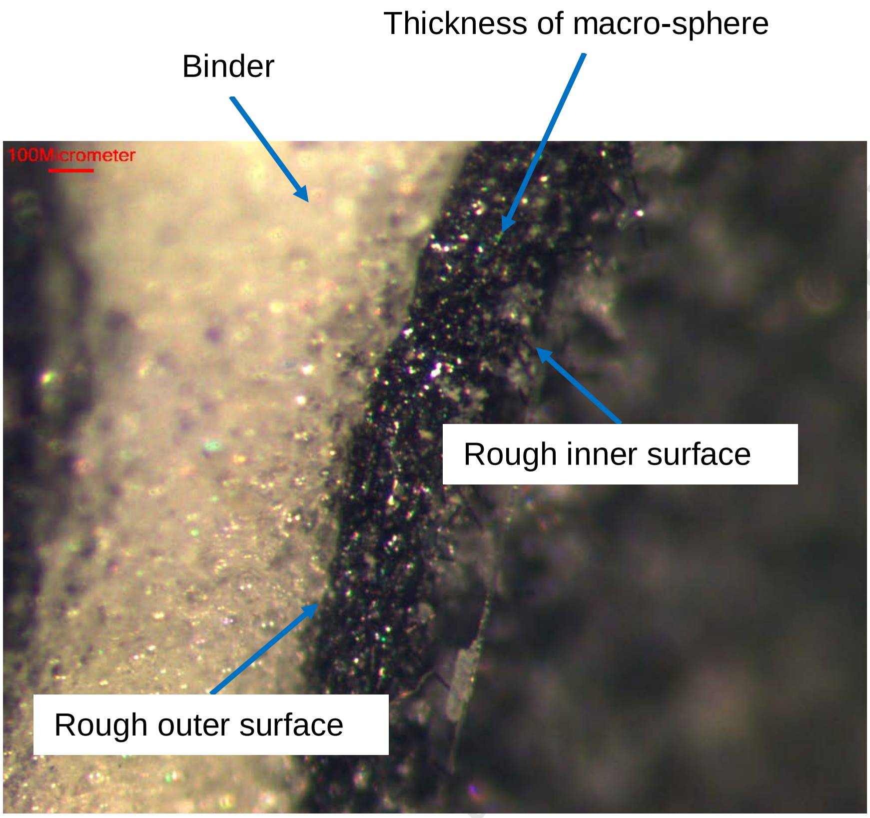
Thickness of macro-sphere
Binder
100Micrometer
Rough inner surface
Rough outer surface

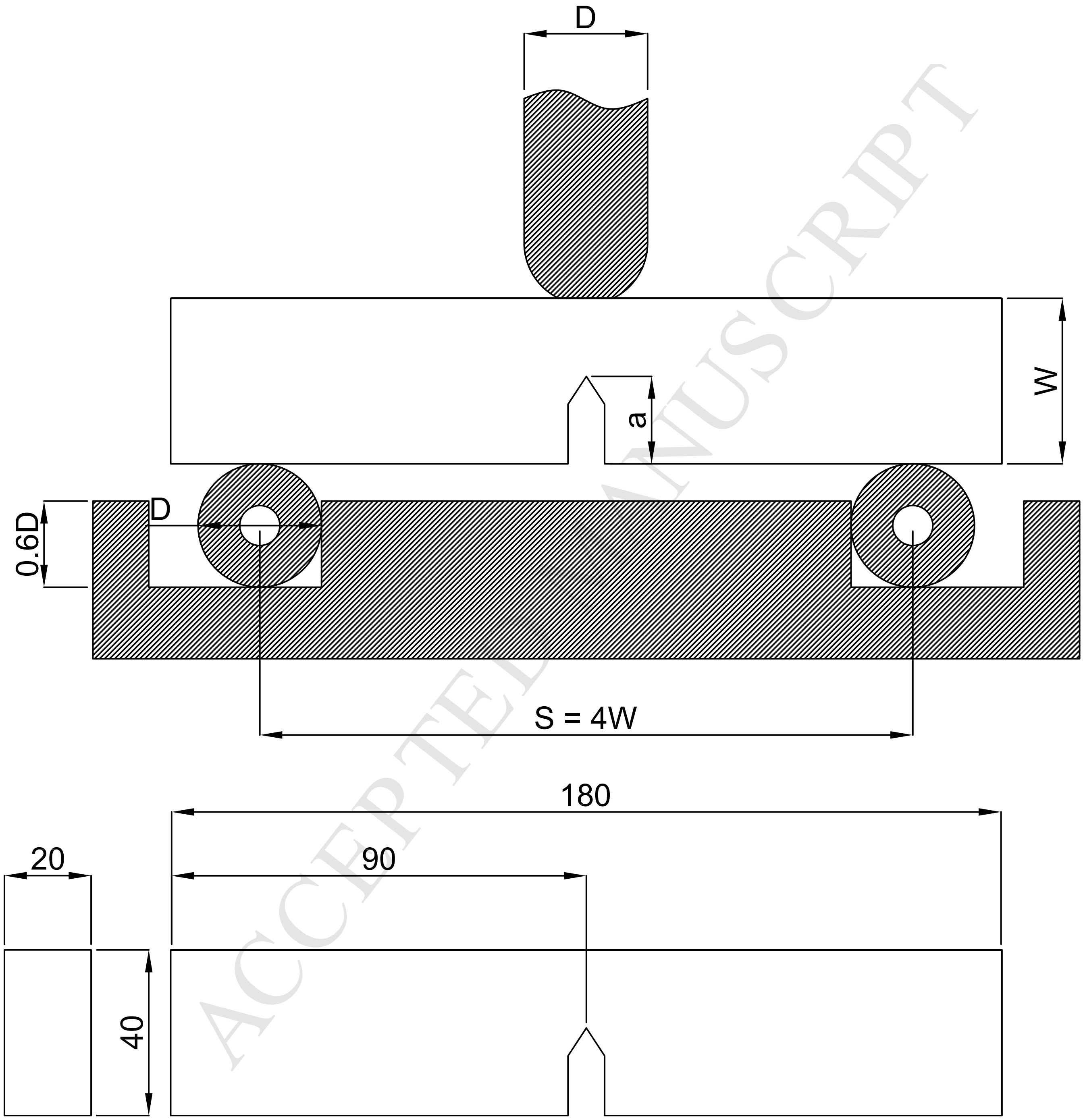
D
W
a
0.6D
D
S = 4W
180
20
90
40

White syntactic foam

Black syntactic foam

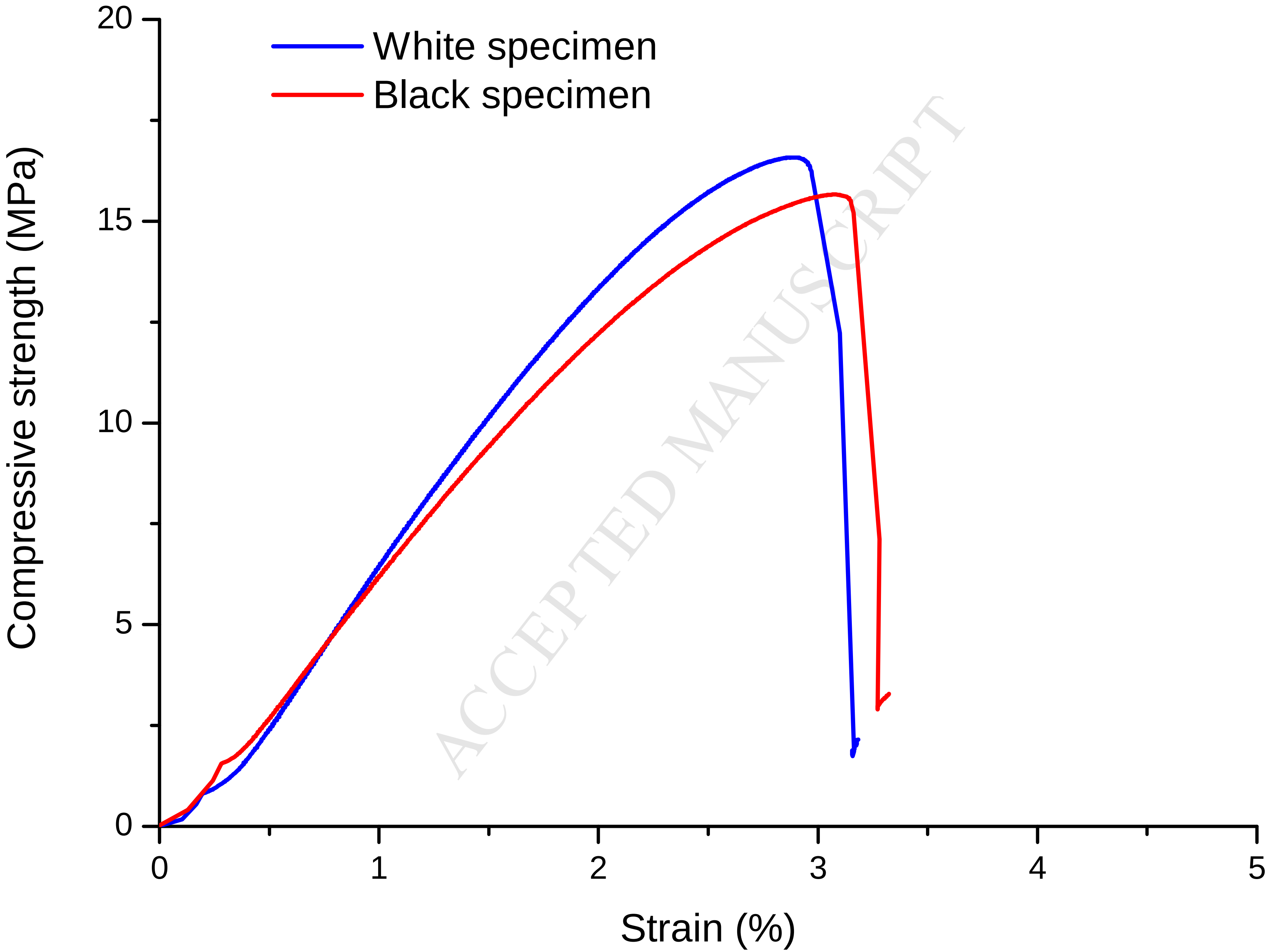

20
15
10
5
0
Compressive strength (MPa)
0
1
2
3
4
5
Strain (%)
White specimen
Black specimen

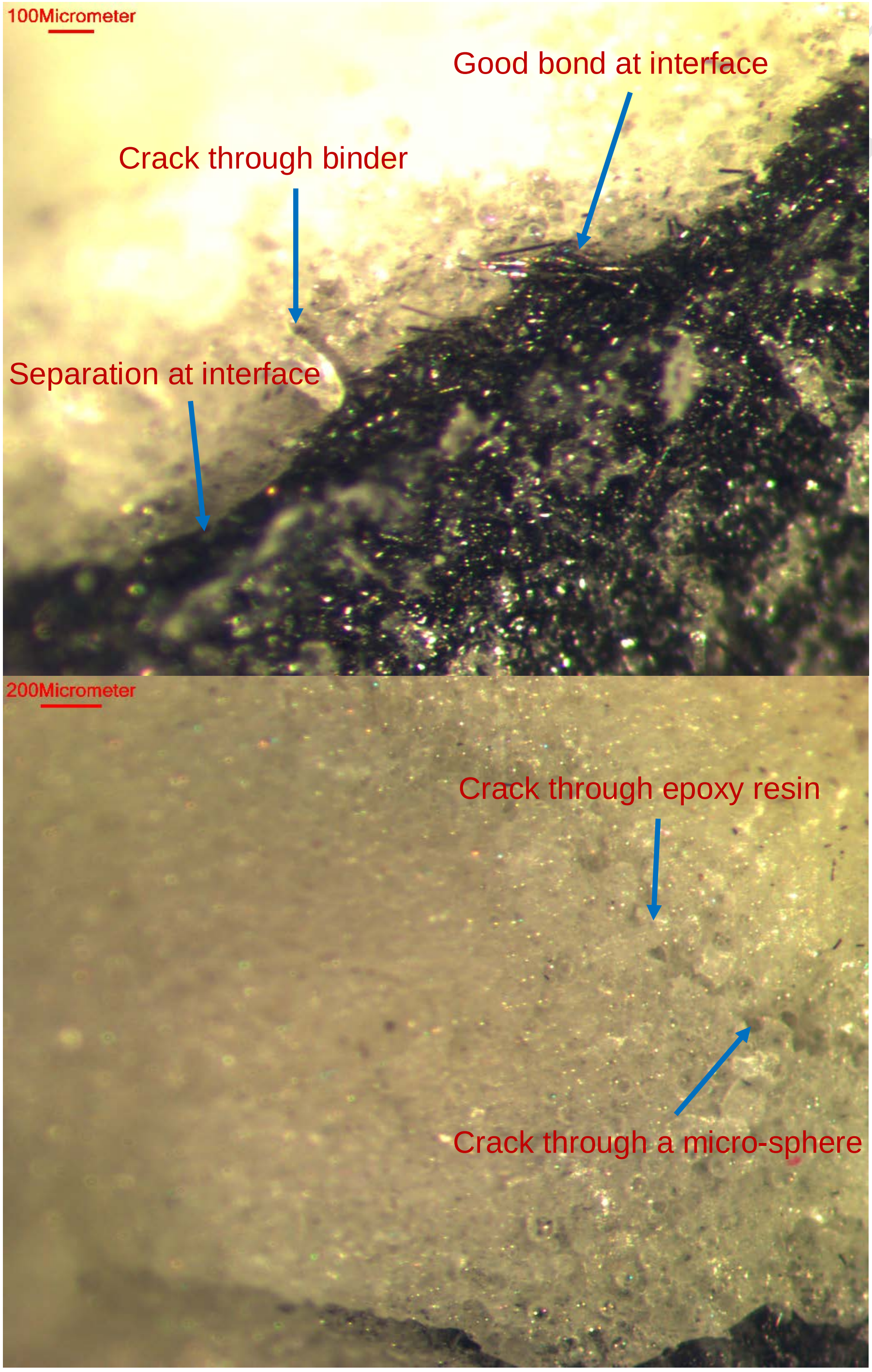
100Micrometer
Good bond at interface
Crack through binder
Separation at interface
200Micrometer
Crack through epoxy resin
Crack through a micro-sphere

HIGHLIGHTS

- Fracture toughness of multiphase syntactic foam
- Impact behavior of multiphase syntactic foam
- Effect of rubber content on mechanical properties
- Impact testing of syntactic foam
- Dynamic properties
- Coating with epoxy resin